

Electrophoretic Deposition of Gentamicin-Loaded Bioactive Glass/Chitosan Composite Coatings for Orthopaedic Implants

Fatemehsadat Pishbin,[†] Viviana Mouriño,^{‡,§} Sabrina Flor,^{‡,§} Stefan Kreppel,^{†,∇} Vehid Salih,^{#,||} Mary P. Ryan,^{*,†,⊥} and Aldo R. Boccaccini^{*,†,∇}

[†]Department of Materials, Imperial College London, Prince Consort Road, London SW7 2BP, United Kingdom

[‡]Department of Pharmaceutical Technology, Faculty of Pharmacy and Biochemistry, University of Buenos Aires, 956 Junín Street, CP1113 Buenos Aires, Argentina

[§]National Science Research Council (CONICET), Buenos Aires, Argentina

[∇]Institute of Biomaterials, Department of Materials Science and Engineering, University of Erlangen-Nuremberg, 91058 Erlangen, Germany

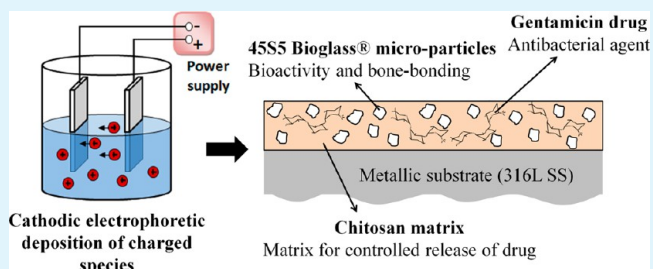
[#]Division of Biomaterials & Tissue Engineering, UCL Eastman Dental Institute, London WC1X 8LD, United Kingdom

[⊥]London Centre for Nanotechnology, Imperial College London, Prince Consort Road, London SW7 2BP, United Kingdom

Supporting Information

ABSTRACT: Despite their widespread application, metallic orthopaedic prosthesis failure still occurs because of lack of adequate bone-bonding and the incidence of post-surgery infections. The goal of this research was to develop multifunctional composite chitosan/Bioglass coatings loaded with gentamicin antibiotic as a suitable strategy to improve the surface properties of metallic implants. Electrophoretic deposition (EPD) was applied as a single-step technology to simultaneously deposit the biopolymer, bioactive glass particles, and the antibiotic on stainless steel substrate. The microstructure and composition of the coatings were characterized using SEM/EDX, XRD, FTIR, and TGA/DSC, respectively. The *in vitro* bioactivity of the coatings was demonstrated by formation of hydroxyapatite after immersion in simulated body fluid (SBF) in a short period of 2 days. High-performance liquid chromatography (HPLC) measurements indicated the release of 40% of the loaded gentamicin in phosphate buffered saline (PBS) within the first 5 days. The developed composite coating supported attachment and proliferation of MG-63 cells up to 10 days. Moreover, disc diffusion test showed improved bactericidal effect of gentamicin-loaded composite coatings against *S. aureus* compared to control non-gentamicin-loaded coatings.

KEYWORDS: coatings, bioactive glass, chitosan, gentamicin, electrophoretic deposition, drug delivery



1. INTRODUCTION

Development of bioactive coatings on metallic orthopaedic implants is an extensive and active research field that is fuelled by the desire for long-term treatment of critical-sized bone defects.¹ The quest for developing the most suitable bioactive implant coating has been addressed from different perspectives: the composition of the bioactive material,² the structure of the coating in terms of being monolithic or composite,³ the surface topography features,⁴ and the fabrication techniques used to prepare the desirable coating.⁵

Among the different bioactive inorganic materials being investigated, silicate bioactive glasses have proved to be a promising group of highly reactive materials as they have been reported to stimulate bone regeneration to a larger extent in comparison to other bioactive ceramics.⁶ Furthermore, combining the bioactive glass structure with a suitable biopolymer has been shown to have advantages such as transforming the brittle glass coating structure into a compliant

and soft composite structure,^{7,8} eliminating high temperatures required for densification of glass coatings and providing a platform for incorporation and release of biomolecules and drugs which often require room temperature processing.^{7,9,10} A well-known biopolymer suitable for biomedical coatings is chitosan, which is a natural polysaccharide consisting of β -(1 \rightarrow 4)-glucosamine and *N*-acetyl-D-glucosamine.¹¹ Chitosan is obtained by *N*-deacetylation of chitin. Notable features of this biopolymer are susceptibility to enzymatic degradation, accelerated angiogenesis, little fibrous encapsulation, ability to link to and deliver growth factors, and improved cellular adhesion.^{11,12}

Despite versatility of methods and compositions, one crucial aspect that needs to be properly addressed when designing

Received: March 18, 2014

Accepted: May 14, 2014

Published: May 14, 2014

orthopaedic coatings, is the ability of the coating material to prevent microbial infections at the implantation site. More importantly, formation of bacterial biofilms should be inhibited as these are considerably resistant to the immune system and to antibiotics.¹³ Because of impaired blood circulation at the bone injury site and low local concentration of drug, systemic drug administration may not be sufficiently effective against bacterial biofilms.¹⁴ Local delivery of drugs via implant coating can be an effective approach to treat infections with high local concentrations of drug, with long-term controlled release and without the risk of systemic toxicity or formation of bacterial biofilms.¹⁵ A broad range of organic and inorganic coating systems with therapeutic capability for orthopaedic applications is being investigated.^{14,16}

Gentamicin sulfate is a broad-spectrum aminoglycosidic antibiotic which is effective against many strains of Gram-negative (e.g., *E. Coli*) and some strains of Gram-positive (e.g., *S. aureus*) bacteria. The molecule of gentamicin can have several components depending on its functional groups and the drug contains different percentages of these components. The most common formula is presented in Figure 1.¹⁷

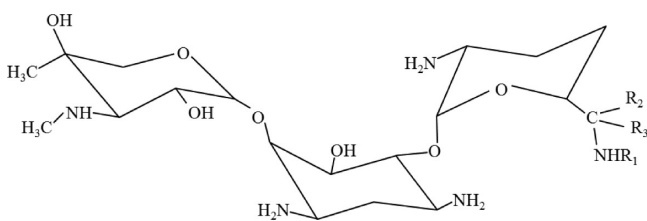


Figure 1. Molecular structure of gentamicin and its different components, C₁: R₁ = R₃ = CH₃, R₂ = H; C_{1a}: R₁ = R₂ = R₃ = H; C₂: R₁ = R₂ = H, R₃ = CH₃; C_{2a}: R₁ = R₃ = H, R₂ = CH₃.

Because of its broad-spectrum action, gentamicin is employed clinically for the treatment of osteomyelitis.¹⁸ As a result, various gentamicin-releasing coating systems have been investigated. For example, stainless steel fracture plates dip-coated with poly(lactic-co-glycolic acid) films containing 20 wt % gentamicin have been successfully applied against *S. aureus*.¹⁹ It has also been observed that biodegradable gentamicin-loaded polyelectrolyte multilayer coatings, developed by layer-by-layer (LBL) deposition, displayed synergistic effect for the treatment of osteomyelitis infection in vivo.²⁰ As an inorganic delivery system, vancomycin, gentamicin, tobramycin, amoxicillin, cefamandol, cephalothin, and carbenicillin have been biomimetically incorporated in carbonated hydroxyapatite (HAp) coatings.²¹ It has been demonstrated that antibiotics with carboxyl groups such as cefamandol, cephalothin and carbenicillin are more prone to bind/chelate with calcium in HAp and therefore have a slower release rate. Gentamicin release from sol-gel HAp spin-coated on Ti alloy has been modelled by three nonlinear mathematical methods.²² The results were indicative of a short initial burst release followed by the diffusion of gentamicin. In another study, Zhou and co-workers²³ have demonstrated that the release of gentamicin from electrochemically deposited chitosan/calcium phosphate coating is controlled by its component ratio and surface topography. Moreover, gentamicin released from electrospun poly(vinyl alcohol)/polyurethane multilayer structures has showed bactericidal effect against both *S. aureus* and *P. aeruginosa* strains.²⁴

Electrophoretic deposition (EPD) is a low-cost technique being increasingly used to fabricate uniform coatings for biomedical applications.³ By utilising EPD, coatings with controlled properties can be produced at room temperature and on complex-shaped and porous structures. In EPD, surface-charged particles or polymer molecules in suspension move toward an oppositely charged electrode (i.e., the substrate) due to an applied electrical field and form a coating.²⁵ Co-deposition of polymers and ceramics is one of the most interesting features of EPD applied to the development of biomaterials.^{3,26} Recently, EPD of chitosan/vancomycin antibiotic²⁷ and chitosan/nanobioactive glass/ampicillin antibiotic²⁸ as drug releasing coatings have been investigated. In another study Patel et al.²⁹ have demonstrated EPD of chitosan-gelatin composites loaded with ampicillin as a model drug and have achieved a rate-controllable drug release by a compositional change in the polymers ratio of the deposited films. EPD have also been used to coat stainless steel cardiovascular stents: one study involves EPD of rapamycin-loaded mesoporous silica nanoparticle/carbon nanotube composite³⁰ and the other has shown EPD of N-nitro-somelatonin-loaded poly(D,L-lactide-co-glycolide) nanoparticles.³¹ But both of these investigations have used other techniques to load nanoparticles with the drug component prior to the EPD step.

We have previously studied in detail the electrophoretic deposition of chitosan,³² 45S5 Bioglass,³³ chitosan/45S5 Bioglass,³⁴ and chitosan/45S5 Bioglass/silver nano-particles³⁵ composite coatings. As outlined above, there are only a few publications investigating the feasibility of EPD in single-step incorporation of drugs in a multifunctional composite film. Therefore, the aim of this study is to explore the addition of an antibacterial function to the chitosan/45S5 Bioglass composite coatings by incorporating an antibiotic and we are keen to demonstrate the potential of EPD as a single-step technique for obtaining such a coating. In this work, co-deposition of the multifunctional chitosan/bioactive glass composite coating with added gentamicin has been investigated. The microstructural characteristics of the coatings and their in vitro bioactivity were studied, and preliminary cellular and antibacterial tests to characterize the biological behavior of films were carried out.

2. EXPERIMENTAL PROCEDURES

2.1. Materials. 45S5 Bioglass powder with nominal composition: 45 SiO₂-24.5 Na₂O-24.5 CaO-6 P₂O₅ (wt %) was used. The particle size was in the range 1.6–26.7 μm with a median particle size of 9.8 μm. Medium molecular weight chitosan with a degree of deacetylation of about 85%, acetic acid (>98%), gentamicin sulfate (BioReagent, 50 mg/mL solution in deionized water) and the reagents used in gentamicin derivatisation procedure were all purchased from Sigma-Aldrich. The gentamicin sulfate was reported to have the following composition C₁ < 45%, C_{1a} < 35%, and C₂ < 30%.³⁶ The following reagents were used to prepare simulated body fluid (SBF) solution:³⁷ NaCl, NaHCO₃, KCl, K₂HPO₄·3H₂O, MgCl₂·6H₂O, CaCl₂, Na₂SO₄, Tris-hydroxymethyl aminomethane and HCl (1.0 M) (all from Sigma-Aldrich).

2.2. Electrophoretic Deposition. Solutions of chitosan (0.5 mg/mL) in 1 vol % acetic acid in water were prepared by magnetic stirring at room temperature for 24 h (pH 3). To prepare composite suspensions, Bioglass® particles were dispersed in the chitosan solution. For gentamicin-loaded coatings, 1 mL of gentamicin sulfate solution was added to 24 mL of the prepared composite suspension to obtain a concentration of 2 mg/mL of the drug. The pH of the suspensions was measured using JENWAY 3510 pH Meter (Essex, UK). It should be noted that according to trial EPD experiments, 0.5 mg/mL was found to be a suitable concentration of chitosan in the

solution to obtain a uniform film. As EPD yield is concentration dependent,²⁵ higher chitosan concentrations resulted in a more viscous solution, and electrophoretic deposition of a large porous volume of polymer rather than a uniform film. Conversely at lower concentrations, enough amount of chitosan was not deposited to provide a uniform matrix for bioactive glass embedment. Therefore, 0.5 mg/mL chitosan was selected for these experiments.

AISI 316L stainless steel (called 316L SS hereafter in this work) is among the most commonly used metals for orthopaedic implant applications.³⁸ Thus, for electrophoretic deposition, 316L SS foils (20 mm × 10 mm × 0.2 mm) were utilized as deposition substrate (cathode). Substrates were washed with deionized water and acetone and were dried prior to deposition. A gold counter electrode was used in the EPD cell. The distance between the electrodes was kept constant at 1.5 cm and the suspensions were gently stirred during deposition by a magnetic stirrer. The constant electric voltage was applied by a Thurlby Thandar Instruments (TTi) EL561 power supply (Cambridgeshire, UK). Chitosan (CS) and chitosan/Bioglass (CS/BG) coatings were also prepared to be compared with chitosan/Bioglass/gentamicin (CS/BG/GS) coatings. The EPD experimental conditions for each coating are outlined in Table 1. After deposition,

Table 1. EPD Parameters for Deposition of Coatings from 0.5 mg/mL Chitosan Solutions

coating type	coating name	Bioglass (mg/mL)	gentamicin sulfate (mg/mL)	voltage (V)	time (s)
chitosan	CS	0	0	10	800
chitosan/Bioglass	CS/BG	5	0	10	400
chitosan/Bioglass/gentamicin	CS/BG/GS	5	2	10	400

the cathodic films were gently rinsed with deionized water, dried and stored in a desiccator until further characterization. It should be noted that because chitosan has a lower density (0.6 g/cm³) than Bioglass (2.7 g/cm³), an EPD coating obtained from chitosan-only solution has a lower deposition yield (deposition weight per area) than that of deposited from a Bioglass-containing suspension. In practice, a reasonable amount of chitosan deposit is required to perform characterizations such as thermogravimetric analysis and infrared spectroscopy. Consequently, the EPD time was doubled for CS films to increase deposition yield. The deposition yield was measured to be 1.5 and 4.4 mg/cm³ for CS and CS/BG coatings, respectively.

2.3. Characterization of Coatings. **2.3.1. Microstructural Characterization.** To study the microstructural features, we used high-resolution scanning electron microscopy (LEO Gemini 1525 SEM). The samples were coated with chromium using EMITECH K575X sputter coater (Emitech Ltd., UK) beforehand to avoid any charging artefacts during imaging. The SEM was fitted with an Oxford Instruments INCA energy-dispersive X-ray spectrometer (EDS) which was used for qualitative elemental analysis of the coatings.

The crystalline state of the material was evaluated with X-ray diffraction (XRD) analysis using PANalytical X'Pert Pro MPD instrument with Cu-K α radiation at 40 kV and 40 mA, applying a step size of 0.04° for the 2 θ range of 5–80° and with a count rate of 50 s per step.

Fourier transform infrared spectroscopy (FTIR) was performed in transmission mode using a PerkinElmer Multiscope spectrometer in the mid-IR region (5000–400 cm⁻¹). For FTIR analysis the coatings were removed from the substrates, mixed and ground with potassium bromide (KBr) at a weight ratio of 1:100 and pressed into pellets (13 mm diameter and 0.8 mm thickness).

In order to estimate the composition of the coatings, they were removed from the substrates and thermogravimetric analysis (TGA) and differential scanning calorimetry (DSC) were performed in air using a simultaneous thermal analyzer (NETZSCH STA 449 C, Germany). A heating rate of 10 °C/min was utilized and three samples were tested per coating condition.

2.3.2. Acellular In Vitro Study by Immersion in Simulated Body Fluid. To investigate the level of acellular in vitro bioactivity of coatings in terms of hydroxyapatite (HAp) formation, the simulated body fluid (SBF) test as proposed by Kokubo et al. was performed.³⁷ Coated samples (10 mm × 10 mm × 0.2 mm) were immersed in 30 mL of SBF and were then incubated at 37 °C for 2, 5, 7, 14, and 21 days. At each time point samples were removed from SBF, rinsed with ion-exchange distilled water, left to dry in air, and then stored in a desiccator. The formation of HAp was examined with SEM/EDX, XRD and FTIR techniques after SBF immersion. For comparison, samples before immersion in SBF were also characterized.

2.3.3. Gentamicin Release Study. To determine the efficiency of EPD to incorporate gentamicin in the chitosan matrix, release of the antibiotic from another type of sample; known as conditioned sample; was also investigated. To prepare the conditioned sample, 100 μ L of gentamicin sulfate solution (2 mg/mL) was pipetted over coatings of CS/BG and samples were left to dry at room temperature. The amount of antibiotic released from these samples was compared with that from EPD samples.

In order to quantify the amount of gentamicin incorporated in the coatings, coatings were scraped off the substrate and immersed in 1 mL deionized water (borate buffer pH 10.4). After 10 min sonication, the immersion samples were centrifuged and the supernatant was tested for dissolved gentamicin.

The in vitro release of gentamicin antibiotic from the EPD and pipetted samples was studied by incubating coated samples (10 mm × 10 mm × 0.2 mm) in 2.5 mL of phosphate buffered saline (PBS, Sigma P4417-50TB, one tablet in 200 mL deionized water) at 37 °C. Aliquots of 2.5 mL (the total release volume) were withdrawn from samples at predetermined times (42 h, 84 h, and 7, 14, 21, 28, 35, 42, 49, and 56 days), and were replenished by adding fresh PBS. The reason PBS solution was used instead of SBF was that the high concentration of ions in SBF limits detection of released gentamicin by the quantification method used here, which is high-performance liquid chromatography (HPLC).

The concentrations of gentamicin incorporated in the supernatant of as-received coatings as well as in the releasing samples were quantified by HPLC and ultraviolet (UV) detection. For this purpose, the gentamicin in solution had to be derivatised. As gentamicin is an aminoglycosidic compound, its derivatisation methods involve chemical reactions with the primary amino groups of the drug.¹⁷ The method described in the following paragraphs has been developed for derivatisation of gentamicin in the present study and is based on modifications to a technique previously proposed by Sampath et al.³⁹

The reactive solution (derivatising agent) consisted of 130 mg of *ortho*-phthalaldehyde dissolved in 0.5 mL of methanol. This solution was mixed with 3.8 mL borate buffer (30 mM, pH 10.4) and 290 μ L 2-mercaptoethanol (as gentamicin derivatizing agent) was added to it. The final volume was adjusted to 5 mL by borate buffer. The obtained reactive solution was kept at 4 °C, in which it was stable for 2–3 days. For derivatisation, 0.4 mL of reactive solution was added to 1 mL of test sample and 1.2 mL of 2-propanol (total volume of 2.5 mL). The solution was then heated in a 40 °C bath for 5 min.

HPLC was performed with a Thermo Scientific spectra SYSTEMS, SCM 1000 instrument (AS3000 autosampler and P4000 Quaternary pump). Separation of the derivatised solution was carried out on a reversed phase C18R column (50 mm × 2 mm, 3 μ m particle size) at a flow rate of 0.3 mL/min, at 20 °C and with the flux of mobile phases as shown in Table 2. The UV detection was performed at 230 nm using Thermo Scientific UV 2000 (dual wavelength) detector. For estimation of the amount of gentamicin, the software HPLC Thermo Scientific Chromatography Data Systems was utilized.

2.4. Biocompatibility Studies. **2.4.1. Microbiological Test.** The effect of the incorporation of gentamicin in coatings on the viable counts of *S. aureus* (ATCC 25923) was investigated by conducting agar disc diffusion tests on CS, CS/BG, and CS/BG/GS EPD samples with 316L SS and PBS as controls. Coatings were first sterilized using UV treatment for 45 min each side. Five samples of each series (10 mm × 10 mm in surface area) were immersed at 37 °C in PBS (5 mL) at pH 7.4 for 10 days. At predetermined time intervals (1, 2, 3, 5, 7,

Table 2. Step Gradient of Mobile Phases Used in HPLC of Gentamicin

time (min)	A (%) ^a	B (%) ^b
0	65	35
4	65	35
6	75	25
60	75	25

^aA is 700 methanol:250 water:50 acetic acid (volume ratio) + 5 g of octansulfonate. ^bB is methanol.

and 10 days) aliquots (5 μ L) of each series were removed and applied to paper discs (6 mm diameter) and placed on the surface of Mueller-Hinton agar plates seeded with *S. aureus* through a modification of the agar disc diffusion method of CLSI M02 A10.⁴⁰ After each aliquot was taken, the remaining volume was replaced with fresh PBS to mimic physiological clearance. Approximately 10⁷ colony-forming units of *S. aureus* were inoculated on Mueller-Hinton agar plates. After 24 h of incubation, the zones of inhibition (diameter of the inhibition circle around paper disks) were measured.

Bacterial inoculate for Mueller-Hinton agar plates seeding was prepared as follows: bacteria were streaked on Trypticase soy agar (Difco, USA) from -70 °C stocks. Overnight agar cultures were transferred to tryptic soy broth (Difco, USA) and statically incubated at 37 °C for 48 h. After centrifugation (8000 \times g, 4 °C, 10 min), bacteria were re-suspended to 1.5×10^8 CFU/mL.

2.4.2. In Vitro Cellular Test. MG-63 osteoblasts (ECACC, UK), a human osteosarcoma cell line, were used to assess in vitro cytocompatibility of CS, CS/BG and CS/BG/GS EPD coatings. Uncoated 316L SS substrate and tissue culture plastic (TCP) were used as controls. Cells were cultured in low glucose (1 g/L) Dulbecco's Modified Eagles Medium (DMEM containing L-Glutamine), supplemented with 10% (v/v) Fetal Bovine Serum (FBS) and 1% (v/v) antibiotic (penicillin/streptomycin) solution (all from PAA, Coelbe, Germany) (which will be referred to as "complete medium"). Prior to testing, the samples (10 \times 10 \times 0.2 mm³) were UV-sterilized for 45 min each side.

Almost confluent (80%) cultures were harvested for experiments with a solution of 0.05%/0.002% Trypsin/EDTA in Ca²⁺/Mg²⁺-free PBS (PAA, Coelbe, Germany) and pelleted by centrifugation at 1000 rpm for 5 min. Cell counting was performed by trypan blue dye and haemocytometer. The test samples were seeded at a density of 20 000 cells/cm² and were incubated in 1 mL of complete medium at 37 °C in a humidified atmosphere (5% CO₂ in 95% air). After an overnight period, samples were transferred to a new well plate and replenished with fresh medium. The cells were then allowed to grow on the coatings for up to 7 days, with the medium changed every 2 days. At specific time intervals, cell proliferation was carried out using the alamarBlue assay (AbD Serotec, Oxford, UK). For this assay, at the end of each time point, 100 μ L of the culture medium was replaced with alamarBlue indicator dye and incubated for 4 h. Sample aliquots of 200 μ L were then taken and its fluorescence was measured at excitation and emission wavelengths of 530 and 590 nm, respectively (Thermo Labsystems Fluoroskan Ascent FL, Waltham, USA). The number of viable cells was estimated by interpolating fluorescence readings from a 6 point standard alamarBlue curve. The standard curve ($R^2 = 0.9902$) was obtained by 1:2 serial dilution of initial 1×10^5 cell number.

The surface attachment of MG-63 cells was qualitatively analysed at day 1 and day 7 by SEM imaging. Samples were removed and fixed in 3% glutaraldehyde in 0.1 M cacodylate buffer overnight at 4 °C. Then the samples were dried by washing in a graded series of ethanol (50, 70, 90, and 100%) and finally critical point dried in hexamethyldisilazane for 2 min. Samples were left to dry in the fume cupboard for 2 h, after which they were attached to aluminum stubs and sputter coated with Cr for SEM.

2.4.3. Data Analysis. For the microbiological assay five samples per coating condition were tested and for the cellular assay two individual experiments each containing coating samples in quadruplicate were

performed. The results were reported as mean \pm standard deviation. One-way analysis of variance (ANOVA) with $p < 0.05$ as significance level was utilized for statistical analysis and Tukey's range test was used for post-hoc analysis. The analyses were carried out using MINITAB 15 statistical software.

3. RESULTS

3.1. Characterization of Coatings. 3.1.1. Microstructural Characterization. The microstructure of the CS/BG/GS coating at low and high magnifications is shown in Figure 2a,

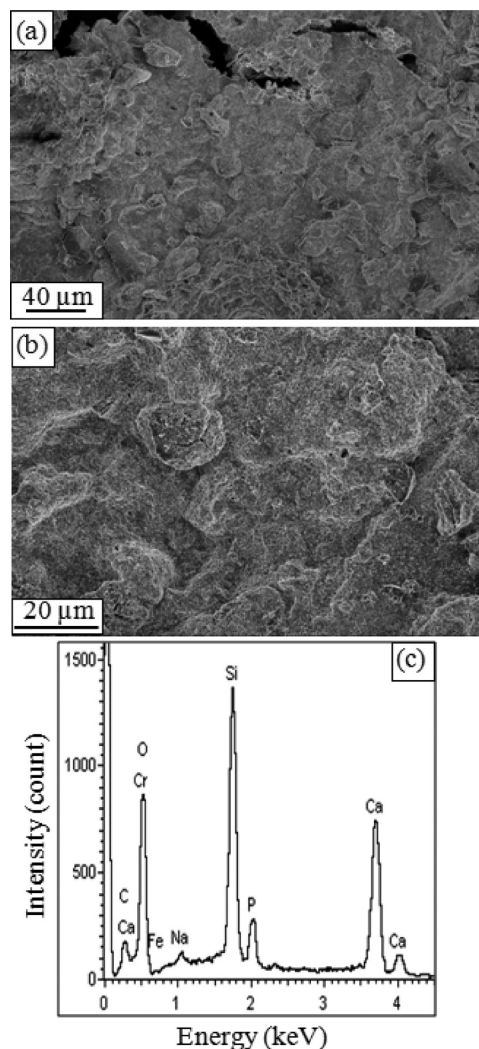


Figure 2. SEM images of CS/BG/GS coating prepared by EPD at (a) lower and (b) higher magnifications; (c) corresponding EDX spectrum.

b. The coating contains a chitosan matrix with micrometer-sized Bioglass® particles embedded in it. Some cracks are also visible in the deposited film. The EDX spectrum (Figure 2c) contains peaks associated with Si, Na, Ca, and P atoms, which are the constituents of Bioglass as well as C atoms, which can be related to the chitosan and gentamicin components of the coating.

FTIR analyses of the EPD coatings are illustrated in Figure 3. The main absorption bands of chitosan as well as the vibration bands for Bioglass® powder are depicted. The most important bands in CS are stretching vibration of O–H from carbohydrate ring and also adsorbed water (3500–3450

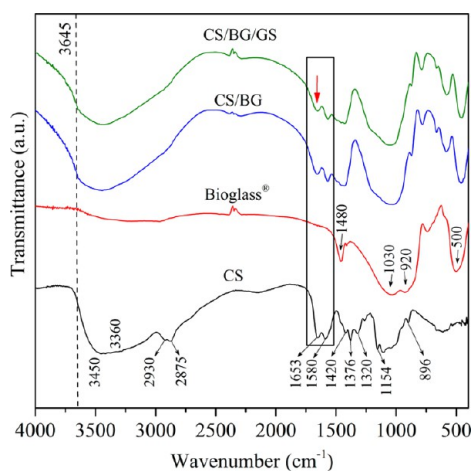


Figure 3. FTIR spectra of Bioglass powder, CS, CS/BG, and CS/BG/GS EPD coatings. The main vibration bands of chitosan and Bioglass are depicted. Formation of a shoulder at 3645 cm^{-1} (dotted line) and the change in relative intensities of 1653 (red arrow) and 1580 peaks in composite films compared to CS film (boxed area) denote formation of hydrogen bonding between bioactive glass particles and chitosan.

cm^{-1}); N–H stretching in amine and amide ($\sim 3360\text{ cm}^{-1}$); vibration of carbonyl bond (C=O) in amide group at 1653 cm^{-1} and N–H bending vibration of amine group at 1580 cm^{-1} .⁴¹ On the other hand, the main bands in the spectrum of pure Bioglass® are attributed to Si–O–Si bending vibration ($\sim 500\text{ cm}^{-1}$) and stretching vibration (920 and 1030 cm^{-1}); the dual peak is indicative of the presence of network modifiers in the structure of glass; i.e., Na and Ca).⁴² The broad peak at 3500 cm^{-1} and the one at 1480 cm^{-1} ; respectively; are associated with water and carbonate groups adsorbed from the atmosphere.

The FTIR spectra of composite CS/BG and CS/BG/GS films (Figure 3) indicate the presence of peaks associated with both chitosan and Bioglass®. More importantly, comparison of the spectra of CS/BG, and CS/BG/GS with that of CS in Figure 3, confirms the presence of the following changes in the composite films: broadening of spectrum in the range $3750\text{--}3000\text{ cm}^{-1}$, formation of O–H shoulder at 3645 cm^{-1} (Figure 3 dashed line) and reduction of C=O vibration at 1653 cm^{-1} relative to N–H vibration at 1580 cm^{-1} (Figure 3 boxed area). All of these changes are attributed to the formation of hydroxyl groups and hydrogen-bonding.⁴³ The suspension of glass particles in aqueous medium leads to formation of free surface hydroxyl groups which can be involved in hydrogen-bonding with chitosan hydroxyl and carbonyl moieties. This hydrogen-bonding results in adsorption of chitosan on glass particles, provides their electrosteric stabilisation in the suspension and in turn aids the co-deposition of the glass and polymer components. Because the main vibration bands of gentamicin molecule are related to N–H and O–H bonds hydrogen bonding between chitosan and gentamicin molecules is also expected. Due to the overlapping of these bands with those of the chitosan structure, the FTIR spectra of CS/BG, and CS/BG/GS coatings in Figure 3 look similar.

The simultaneous thermal analyses (STA) of the coatings (Figure 4) encompass subsequent stages of moisture evaporation (below $100\text{ }^{\circ}\text{C}$) and combustion of chitosan (in the range $220\text{--}600\text{ }^{\circ}\text{C}$). The DSC data of CS coating has two exothermic peaks at ~ 300 and $\sim 500\text{ }^{\circ}\text{C}$ corresponding to a

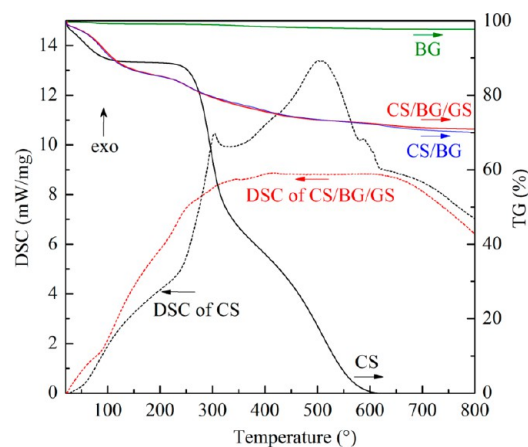


Figure 4. TGA and DSC curves comparing Bioglass powder (BG), CS, CS/BG, and CS/BG/GS EPD coatings, showing the weight loss due to water evaporation and burning out of chitosan.

two-stage thermal decomposition of chitosan.^{34,44} Gentamicin is also expected to thermally decompose in these stages. The TGA curve of the as-received Bioglass powder (BG) shows about 3% weight loss due to loss of moisture and hydroxyl groups. The comparison of TG curves reveals that the percentage of weight loss in both gentamicin-containing and non-containing coatings is notably less than in CS coating because of the presence of glass particles. Because of the lower amount of chitosan in the CS/BG and CS/BG/GS films, their TGA curves do not display the second stage of chitosan burning out as clearly as in neat CS coating. For the same reason chitosan burning produced less pronounced exothermic peaks in the DSC curve of CS/BG/GS compared to DSC curve of CS. The amount of glass particles in CS/BG and CS/BG/GS is $70.03 \pm 0.05\text{ wt } \%$ and $70.93 \pm 0.07\text{ wt } \%$; respectively, which is indicative of almost similar loading of particles in both cases.

3.1.2. Acellular in Vitro Study in SBF. Incubation of CS/BG/GS coatings in SBF at $37\text{ }^{\circ}\text{C}$ provided evidence of bioactivity of the developed gentamicin-loaded coatings. As the SEM images and the EDX spectrum of a sample after 14 days of SBF immersion show (Figure 5), SBF immersion has led to formation of some pores in the structure of the coating and a newly formed nanostructured layer has covered the sample. The EDX spectrum also demonstrates an increase in the intensity of P and Ca peaks and a decrease in the Si peak intensity compared to the as-received samples (Figure 2c), which is associated with deposition of a calcium and phosphorous-rich phase. The new phase also contains small amount of Mg.

Furthermore, XRD and FTIR results obtained from SBF treated samples support the formation of the new phase as soon as 2 days of SBF incubation. The XRD patterns (Figure 6) show that at day 2 a semicrystalline phase with main peaks at 32° and 25.8° has developed. The crystalline structure of the new phase exhibits XRD peaks matching those of the standard pattern of hydroxyapatite (HAp) crystals (ICDD 00-001-1008). According to the Supporting Information (Table S1), the analysis of full width at half maximum of the XRD peak from (1122) crystallographic plane ($2\theta \approx 32.5^{\circ}$) shows that the average crystallite size has increased from 4.2 nm at day 2 to 5.3 nm at day 21 of SBF immersion. Additionally the peak area has increased from day 2 to day 21 suggesting a higher proportion

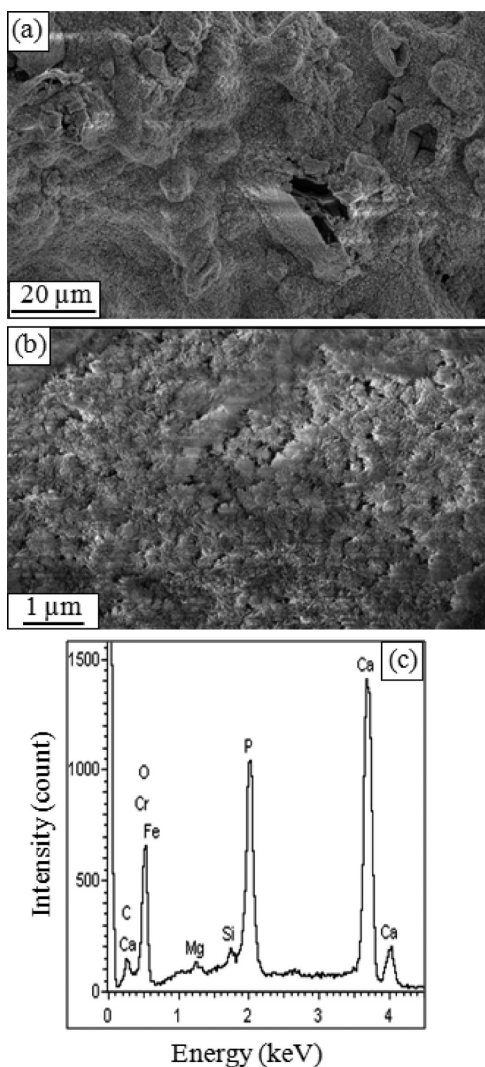


Figure 5. SEM images of CS/BG/GS EPD coating at (a) lower and (b) higher magnifications and (c) EDX analysis after 14 days treatment in SBF. The electron charging in the SEM images is due to the porous nature of the newly formed phase.

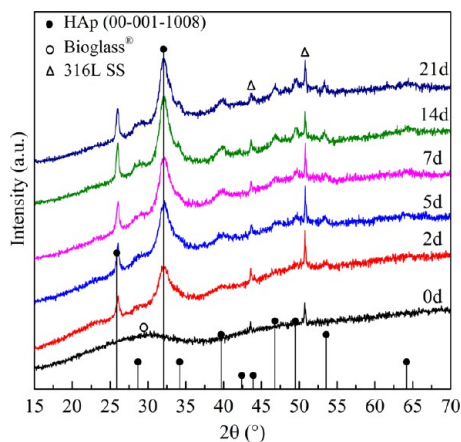


Figure 6. XRD patterns of CS/BG/GS EPD coatings before (0 days) and after treatment in SBF for 2, 5, 7, 14, and 21 days. The standard pattern for HAp (00-001-1008) has been shown for comparison.

of newly formed crystalline HAp phase at longer SBF immersion times.

The FTIR spectra of the corresponding SBF samples presented in Figure 7 display a reduction in the heights of

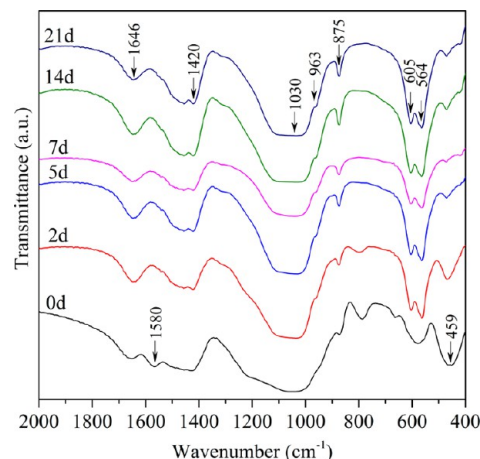


Figure 7. FTIR spectra of CS/BG/GS EPD coatings before (0 days) and after treatment in SBF for 2, 5, 7, 14, and 21 days.

the peaks related to Bioglass (Si–O–Si at 459 cm^{-1}) and chitosan (amine at 1580 cm^{-1}) with SBF immersion time. Depicted graphs also show formation of new bonds within 2 days, which is coherent with XRD data. Occurrence of phosphate (564 , 605 , 963 , and 1030 cm^{-1}) and carbonate (875 and 1420 cm^{-1}) peaks evidences the formation of hydroxyl carbonate apatite (HCAp). The vibration at 1646 cm^{-1} is due to adsorbed water in the structure of the new phase.

3.1.3. Gentamicin Release Study. The amounts of the loaded and released gentamicin were evaluated by HPLC-UV technique after the derivatisation procedure. An example of the chromatographs obtained is presented in Figure 8. Assessment

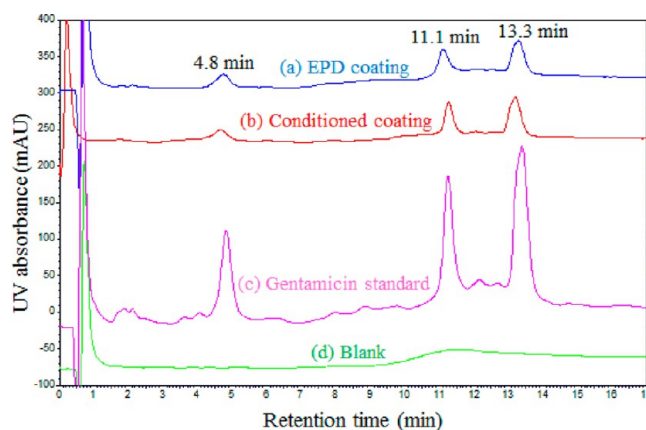


Figure 8. Chromatographs of gentamicin released from (a) EPD and (b) conditioned CS/BG/GS coatings, in comparison to the (c) standard gentamicin solution and (d) blank (PBS) samples. The retention times for EPD coatings are displayed.

of HPLC peaks in EPD and conditioned samples in comparison to the blank and standard, provides evidence for gentamicin quantification. According to the graphs, the retention times of different gentamicin components are approximately 4.8, 11.1, and 13.3 min, respectively, with slight shifting in different samples. Identification of these three gentamicin components,

however, would require further investigations such as mass spectroscopy, which was beyond the scope of this study.

The amount of gentamicin loaded in 1 cm^2 (substrate area) of EPD and conditioned samples were $144.2 \pm 0.8 \mu\text{g}$ and $219 \pm 1 \mu\text{g}$, respectively. As 50 mg of gentamicin sulfate was added to the EPD suspension, it can be concluded that 0.3% of the drug in the suspension was deposited in the EPD sample.

Gentamicin release profiles from both EPD and conditioned samples are depicted in Figure 9. Although for the EPD sample

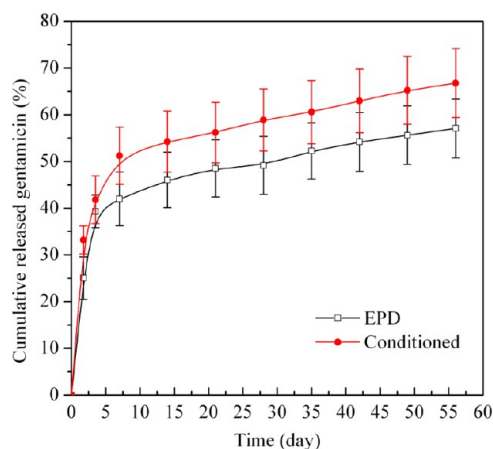


Figure 9. Cumulative release of gentamicin from EPD and conditioned CS/BG/GS coatings in PBS (The data indicate mean \pm standard deviation for three individual experiments).

nearly 50% of the loaded antibiotic was released within 28 days of immersion in PBS, a similar release percentage was reached after 7 days for the conditioned sample. After the initial burst release, the concentration of the drug in the medium increased slowly up to 56 days and reached up to 57.1% ($82.31 \mu\text{g}$) and 66.7% ($146.12 \mu\text{g}$) for EPD and conditioned samples, respectively. Overall, the release rate of gentamicin from the composite films was lower for the EPD coatings.

3.2. Biocompatibility Studies. **3.2.1. Microbiological Study.** The antimicrobial disc susceptibility test indicated that the medium from CS/BG/GS coatings subjected to immersion in PBS developed a zone of inhibition of about 13 mm up to 2 days (Figure 10). A significant difference was observed between CS/BG/GS and CS/BG films for the first 2 days during which the burst release of gentamicin takes place. However, after 2 days both CS/BG and CS/BG/GS films were capable to inhibit bacterial growth at a significantly lower level (5.4–6 mm). This secondary, low efficiency bacteriostatic effect, which can also be observed in CS/BG samples from day 1, can be related to the local increase in pH during the degradation of Bioglass.⁴⁵ The increase in pH in the immediate environment around bioactive glass particles has been reported by other researchers.⁴⁶ The PBS control samples, 316L SS and CS coatings, did not develop any zone of inhibition against *S. aureus* growth.

3.2.2. In Vitro Cellular Study. The cellular metabolic activity was measured by alamarBlue assay and based on these results, the percentage of cell number was estimated. As Figure 11 shows, CS, CS/BG, CS/BG/GS, and controls (316L SS and TCP) supported proliferation of MG-63 cells over 7 days. At each time point, all coatings exhibit significantly ($p < 0.05$) smaller cell number compared to TCP (positive control). After 7 days of culture, no significant difference was observed among 316L SS, CS, CS/BG and CS/BG/GS samples. It was observed

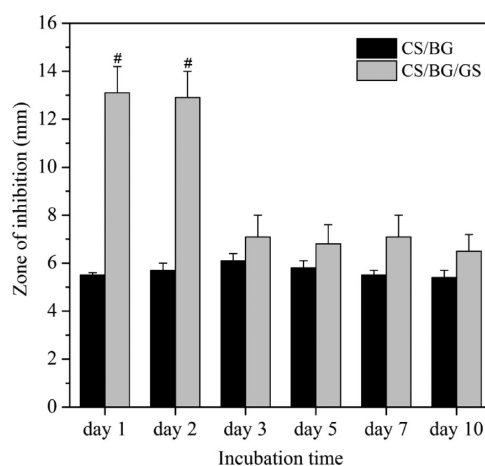


Figure 10. Antimicrobial disc susceptibility test showing the relative diameters of zones of inhibition after different periods of immersion in PBS up to 10 days. The PBS control, 316L SS, and CS did not develop any zones of inhibition. ($p < 0.05$ at the same time period: # is for CS/BG/GS vs. CS/BG coatings) (The data represent mean \pm standard deviation for five individual experiments).

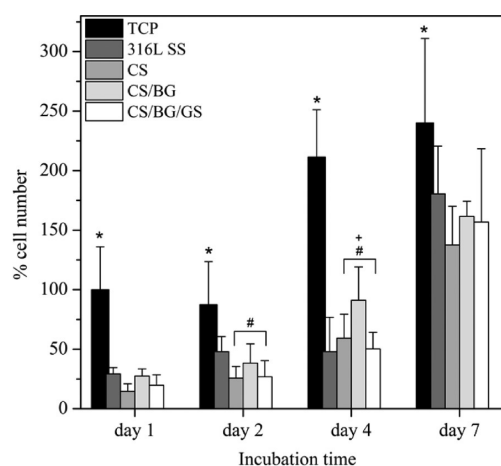


Figure 11. Osteoblast-like human osteosarcoma cell line (MG-63) response to 316L SS substrate, CS, CS/BG and CS/BG/GS coatings measured by alamarBlue assay up to 7 days culture. Tissue culture plastic (TCP) was used as control. The resultant number of cells for each coating was normalised against the number of cells on TCP at day 1 culture and was reported as percentage. $p < 0.05$ at the same time period: * is for TCP vs. all other coatings; # is for marked bar vs. 316L SS; + is for marked bar vs. CS/BG. (Data represent the mean \pm standard deviation of two individual experiments each performed in quadruplicate).

that the proliferation of cells on all samples increased over the period of study. The results indicate that the gentamicin-loaded coatings were nontoxic to cells.

Electron microscopy images of samples subjected to cell culture study show evidence of MG-63 cells attachment to different coatings. For example, Figure 12 shows cells spreading over samples, which is seen to increase from day 1 to day 7. In addition, on 316L SS and CS samples confluent cells were observed at day 7 (Figure 12b, d). These results confirm that the EPD coatings supported attachment and growth of osteoblast-like cells over 7 days in culture.

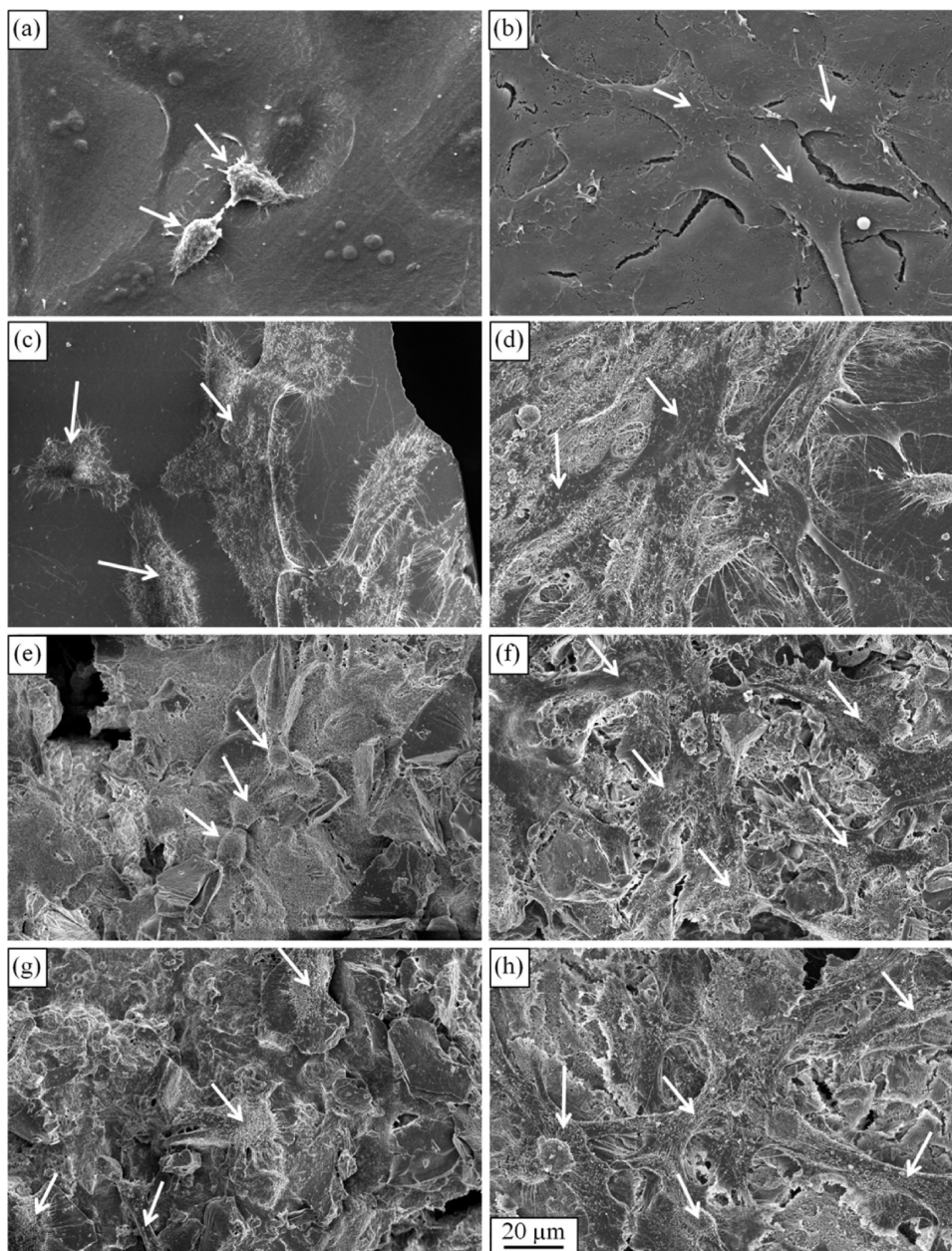
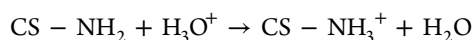


Figure 12. SEM images showing morphology of MG-63 cells spreading on the surface of (a, b) 316L SS, (c, d) CS, (e, f) CS/BG, and (g, h) CS/BG/GS at (a, c, e, g) day 1 and (b, d, f, h) day 7 of culture (some of the cells are marked with white arrows).

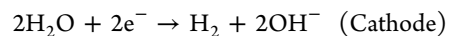
4. DISCUSSION

In this work, EPD was successfully used to deposit a multifunctional coating on a metallic substrate. Although 316L SS was used here as deposition substrate, it is pertinent to point out that for similar substrate surface conditions, as long as the substrate is electrically conductive, the EPD rate is independent of the substrate material.²⁵ Therefore, the methodology applied here is extendable to other conductive implant substrate materials such as Ti alloys.

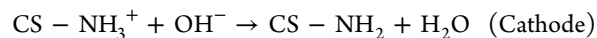
We have previously explained in detail the EPD mechanisms of chitosan³² and bioactive glass.³³ Chitosan macromolecules dissolve in acidic aqueous solution ($\sim\text{pH} < 5$) due to protonation of amine groups and form polycations



Moreover, during the EPD process, electrolysis of water occurs that increases the local pH at the cathode



Consequently, as the electrophoresis of polycations towards the cathode occurs, the protonated amine groups of chitosan lose their charge in the high pH region to form an insoluble deposit



On the other hand, bioactive glass particles develop a pH-dependent surface charge due to surface-bound hydroxyl groups.⁴⁷ At pH below the isoelectric point of Bioglass (pH 11.5), the concentration of positive surface charges is more than the negative ones and a net positive surface charge is obtained. These particles are moved toward the cathode by the electric field and form a deposit by coagulation.³³

FTIR analyses confirmed the hypothesis that during the electrophoretic deposition process, positively charged chitosan molecules in suspension interacted with the hydroxyl groups on the bioactive glass particles surface to form hydrogen-bonds. This phenomenon, which leads to adsorption of chitosan on glass particles, improves the stability of Bioglass® suspensions through electrosteric stabilisation²⁶ and leads to electrophoretic co-deposition of the polymeric and glass components. Due to relatively larger concentration of glass particles in the EPD suspension (5 mg/mL) compared to the chitosan concentration (0.5 mg/mL), a higher wt % of bioactive glass (~70 wt %) is incorporated in the final coating.³⁴ Moreover, the alkaline effect caused by Bioglass partial dissolution in the chitosan solution, renders lower charge density of chitosan chains as well as higher suspension conductivity and consequently lower deposition rate of the polymer is achieved.³² These two factors result in formation of a more brittle EPD coating with increasing glass concentration, which is more susceptible to cracking upon drying. Furthermore, water electrolysis and hydrogen gas production at the cathode during EPD leaves porosity in the structure. The surface topography of chitosan film changes with the amount of bioactive glass particles incorporated in it. Results not presented here show an increase in surface roughness with higher Bioglass content as well as deposition of a smoother composite film when nanosized Bioglass particles were used.⁴⁸

To add antibacterial functionality to these composite coatings, we introduced gentamicin sulfate into the EPD suspension. Gentamicin has high water solubility and the pK_a values of amino groups of gentamicin are between 5.5 and 9; hence at acidic pH the drug molecule is positively charged.⁴⁹ Therefore, it was anticipated that cathodic deposition of the drug from the composite suspension would be feasible. Moreover its stability over a broad pH range (2–10) up to 15 days has been reported.⁵⁰ This facilitates incorporation of the drug in the acidic pH of chitosan/Bioglass suspension (pH 4.46 ± 0.02) used in the present EPD experiments. Additionally, the presence of amino and hydroxyl groups in the gentamicin molecule can lead to the formation of hydrogen bonds with the hydroxyl moieties of Bioglass and chitosan.⁵¹

EDX measurements indicated that the HCAp surface layer developed on CS/BG/GS composite coating after immersion in SBF had a Ca/P atomic ratio of 1.56 ± 0.04 . The slightly lower Ca/P atomic ratio in this study compared to that of bone mineral (Ca/P = 1.57 to 1.62)⁵² may be due to the substitution of Mg atoms in the HAp structure. Furthermore, the test was not conducted in equilibrium with CO₂ atmosphere, which is a requirement for physiological conditions. Such factors can result in formation of a calcium-deficient apatite with lower Ca/P ratios.^{52,53} Although HAp-forming ability in SBF has been widely assumed as an indication of bioactivity *in vivo*,³⁷ the SBF test according to Kokubo³⁷ has been discussed critically in the literature⁵⁴ and improvements for *in vitro* bioactivity testing have been suggested. Under these considerations, the SBF testing in this work has been conducted to demonstrate the HAp-forming ability of Bioglass-containing antibacterial composite coating based on the standardised Kokubo method, which enables a comparison with a large volume of data in the literature.

One of the complexities associated with gentamicin is its quantification by HPLC. As this aminoglycoside is a weak UV chromophore, it needs to be post-column derivatised to be detectable by UV. Most derivatisation techniques involve

chemical reaction with amino groups of the drug.¹⁷ The method developed here utilizes *o*-phthalaldehyde in the presence of 2-mercaptoethanol as derivatising. It has been shown that this chemical combination can significantly improve derivatisation of primary amino groups compared to other chemicals such as ninhydrin or fluorescamine and therefore provides higher detection sensitivity.⁵⁵

Drug release kinetics from a polymer containing matrix depends on various factors such as polymer swelling and erosion, drug distribution inside the matrix and matrix porosity.⁵⁶ As the present coatings have pores and a low weight percentage of chitosan, the characteristic time of diffusion of the solvent is short and consequently drug release can be mainly influenced by drug dissolution and diffusion in the liquid which fills the pores. Additionally it has been demonstrated that for a uniform drug distribution the dissolution of the drug at the matrix/release medium interface gives rise to a burst effect followed by a slower release.⁵⁶ The release profiles from both EPD and conditioned samples were found to follow this trend. Because conditioned samples have higher total amount of loaded drug as compared to EPD samples; with most of it expected to be physically bound to the surface layer; both stages of release occurred faster. Moreover, this feature displays the efficiency of EPD in incorporation of the drug within the coating rather than on the coating surface. On the other hand, the amount of incorporated drug via EPD has been relatively low which might be due to the low electrophoretic mobility of gentamicin molecule at the suspension pH (~4.5). Therefore, additional strategies should be implemented to increase the drug loading capacity in the electrophoretically deposited coatings. These approaches can make use of functionalized glass particles surface with negatively charged chemical groups, which can form strong bonds with cationic gentamicin molecules, thus enhancing its loading efficiency.⁵⁷

S. aureus is the pathogen that is responsible for about two thirds of chronic osteomyelitis infections.²⁰ Most of the bacteria involved in chronic osteomyelitis are susceptible to gentamicin.¹⁸ Gentamicin release from CS/BG/GS films did develop a zone of inhibition against *S. aureus* up to 2 days, which according to CLSI M02 A10⁴⁰ is indicative of an intermediate *S. aureus* susceptibility level. Gentamicin binds to components in the bacterial cell and causes production of abnormal proteins which have a bacteriocidal effect.⁵⁸ To maintain this effect for longer periods of time, the amount of loaded gentamicin and its release profile must be modified so that the initial burst release is prolonged and “more drug” is available for release in later stages. As a potential future step, it is proposed to develop a “sequential drug delivery system” with different release profiles, which can be achieved through deposition of a multilayered coating. In such a system, an outer drug-loaded layer can support initial burst release up to the minimum inhibitory concentration (MIC) and extra drug-containing layers underneath can maintain the MIC for the period of treatment. Ti rods coated with polyelectrolyte films loaded with gentamicin have been reported to release 70% of their drug within 3 days and have delivered a total average of $550 \mu\text{g}/\text{cm}^2$ drug within 4 weeks.²⁰ These films could successfully inhibit *S. aureus* growth *in vitro* and *in vivo*. The corresponding amount of gentamicin loaded in the EPD coatings in this study supported proliferation of osteoblast-like cells in line with chitosan and chitosan/bioactive glass films. After 7 days of culture no significant difference was observed between the samples. This

implies that the present multi-functionalization process of adding bioactive glass particles and gentamicin antibiotic has not compromised the cytotoxicity level of the composite coatings. Thus, the biocompatibility experiments conducted on the EPD samples provide a preliminary assessment of the response of these orthopaedic composite coatings to specific strains of bacteria and to osteoblast cells.

5. CONCLUSIONS

Electrophoretic deposition was applied to prepare bioactive and antibacterial chitosan-based composite coatings for orthopaedic implants. The strategy implemented for multi-functionalizing these coatings involved addition of bioactive glass particles and gentamicin as a molecular antibacterial agent. The coatings formed bonelike apatite upon immersion in simulated body fluid, which is a qualitative confirmation of their bioactivity. Moreover, the coating released 40% of its gentamicin payload within 5 days of burst release followed by a sustained drug delivery over a period of 8 weeks. The release kinetics could inhibit bacterial growth for the first 2 days and it could support cellular proliferation for up to 10 days. To further extend the bactericidal behavior of these coatings, chemical functionalization of glass particles and application of a sequential (e.g. multi-layered) release system are suggested. Future work will explore the suitable range of gentamicin loading which provides a minimum inhibitory concentration against bacteria as well as supporting cellular attachment and proliferation. Additionally, prior to in vivo studies, the interfacial bonding of these coatings to the metallic substrate and the mechanical properties of the developed films will be investigated.

■ ASSOCIATED CONTENT

Supporting Information

Table S1 shows the change in full width at half maxima (FWHM), peak positions and peak areas of (11 $\bar{2}$ 2) crystallographic plane, as well as hydroxyl apatite crystallite sizes at different SBF immersion times. This material is available free of charge via the Internet at <http://pubs.acs.org/>.

■ AUTHOR INFORMATION

Corresponding Authors

*E-mail: m.p.ryan@imperial.ac.uk

*E-mail: aldo.boccaccini@ww.uni-erlangen.de

Present Address

^{||}Plymouth University Peninsula Schools of Medicine and Dentistry, C402, Portland Square, Drake Circus, Plymouth, Devon, PL4 8AA, UK

Notes

The authors declare no competing financial interest.

■ ACKNOWLEDGMENTS

F.P. thanks Imperial College London for granting a scholarship under the Overseas Research Students Awards Scheme (ORSAS). She also thanks Mr. Mohamed H. Parkar (Eastman Dental Institute, UCL, London, UK) for providing training on cellular experiments. The authors also acknowledge Dr. Nicola Mordan (Eastman Dental Institute, UCL, London, UK) for processing and SEM imaging of cells and Mr. Richard Sweeney (Imperial College London, UK) for assistance with TGA tests. The authors are grateful to Dr. I. Thompson (Kings College London, UK) for supplying the Bioglass powder.

■ REFERENCES

- (1) Duan, K.; Wang, R. Surface Modifications of Bone Implants through Wet Chemistry. *J. Mater. Chem.* **2006**, *16*, 2309–2321.
- (2) Wang, G.; Zreiqat, H. Functional Coatings or Films for Hard-Tissue Applications. *Materials* **2010**, *3*, 3994–4050.
- (3) Boccaccini, A. R.; Keim, S.; Ma, R.; Li, Y.; Zhitomorsky, I. Electrophoretic Deposition of Biomaterials. *J. R. Soc., Interface.* **2010**, *7*, S581–S613.
- (4) Khang, D.; Lu, J.; Yao, C.; Haberstroh, K. M.; Webster, T. J. The Role of Nanometer and Sub-Micron Surface Features on Vascular and Bone Cell Adhesion on Titanium. *Biomaterials* **2008**, *29*, 970–983.
- (5) Sola, A.; Bellucci, D.; Cannillo, V.; Cattini, A. Bioactive Glass Coatings: a Review. *Surf. Eng.* **2011**, *27*, 560–572.
- (6) Jones, J. R. Review of Bioactive Glass: From Hench to Hybrids. *Acta Biomater.* **2013**, *9*, 4457–4486.
- (7) Chen, Q. Z.; Blaker, J. J.; Boccaccini, A. R. Bioactive and Mechanically Strong Bioglass®-Poly(D,L-Lactic Acid) Composite Coatings on Surgical Sutures. *J. Biomed. Mater. Res., Part B* **2006**, *2*, 354–363.
- (8) Kim, J.-J.; Won, J.-E.; Shin, U. S.; Kim, H.-W. Improvement of Bioactive Glass Nanofiber by a Capillary-Driven Infiltration Coating with Degradable Polymers. *J. Am. Ceram. Soc.* **2011**, *94*, 2812–2815.
- (9) Rezwani, K.; Chen, Q. Z.; Blaker, J. J.; Boccaccini, A. R. Biodegradable and Bioactive Porous Polymer/Inorganic Composite Scaffolds for Bone Tissue Engineering. *Biomaterials* **2006**, *27*, 3413–3431.
- (10) Nijhuis, A.; Leeuwenburgh, S.; Jansen, J. Wet-Chemical Deposition of Functional Coatings for Bone Implantology. *Macromol. Biosci.* **2010**, *10*, 1316–1329.
- (11) Di Martino, A.; Sittinger, M.; Risbud, M. V. Chitosan: A Versatile Biopolymer for Orthopaedic Tissue-Engineering. *Biomaterials* **2005**, *26*, 5983–5990.
- (12) Muzzarelli, R. A. A. Chitosan Composites with Inorganics, Morphogenetic Proteins and Stem Cells, for Bone Regeneration. *Carbohydr. Polym.* **2011**, *83*, 1433–1445.
- (13) Davies, D. Understanding Biofilm Resistance to Antibacterial Agents. *Nat. Rev. Drug Discovery.* **2003**, *2*, 114–122.
- (14) Goodman, S. B.; Yao, Z.; Keeney, M.; Yang, F. The Future of Biologic Coatings for Orthopaedic Implants. *Biomaterials* **2013**, *34*, 3174–3183.
- (15) Porter, J. R.; Ruckh, T. T.; Popat, K. C. Bone Tissue Engineering: A Review in Bone Biomimetics and Drug Delivery Strategies. *Biotechnol. Prog.* **2009**, *25*, 1539–1560.
- (16) Simchi, A.; Tamjid, E.; Pishbin, F.; Boccaccini, A. R. Recent Progress in Inorganic and Composite Coatings with Bactericidal Capability for Orthopaedic Applications. *Nanomedicine* **2011**, *7*, 22–39.
- (17) Grahek, R.; Zupancic-Kralj, L. Identification of Gentamicin Impurities by Liquid Chromatography Tandem Mass Spectrometry. *J. Pharm. Biomed. Anal.* **2009**, *50*, 1037–1043.
- (18) Farrar, D.; Benson, R.; Milner, R. In *Drug-Device Combination Products: Delivery Technologies and Applications*; Lewis, A., Ed.; Woodhead Publishing Limited: Cambridge, UK, 2010; Chapter 8, pp 190–211.
- (19) Price, J.; Tencer, A.; Arm, D.; Bohach, G. Controlled Release of Antibiotics From Coated Orthopedic Implants. *J. Biomed. Mater. Res.* **1996**, *30*, 281–286.
- (20) Moskowitz, J. S.; Blaisse, M. R.; Samuel, R. E.; Hsu, H. P.; Harris, M. B.; Martin, S. D.; Lee, J. C.; Spector, M.; Hammond, P. T. The Effectiveness of the Controlled Release of Gentamicin from Polyelectrolyte Multilayers in the Treatment of Staphylococcus Aureus Infection in a Rabbit Bone Model. *Biomaterials* **2010**, *31*, 6019–6030.
- (21) Stigter, M.; Bezemer, J.; de Groot, K.; Layrolle, P. Incorporation of Different Antibiotics into Carbonated Hydroxyapatite Coatings on Titanium Implants, Release and Antibiotic Efficacy. *J. Controlled Release* **2004**, *99*, 127–137.
- (22) Aves, E. P.; Estevez, G. F.; Sader, M. S.; Sierra, J. C. G.; Yurell, J. C. L.; Bastos, I.; Soares, G. Hydroxyapatite Coating by Sol-Gel on Ti

6Al-4V Alloy as Drug Carrier. *J. Mater. Sci.: Mater. Med.* **2009**, *20*, 543–547.

(23) Zhou, J.; Cai, X.; Cheng, K.; Weng, W.; Song, C.; Du, P.; Shen, G.; Han, G. Release Behaviors of Drug Loaded Chitosan/Calcium Phosphate Coatings on Titanium. *Thin Solid Films* **2011**, *519*, 4658–4662.

(24) Sirc, J.; Kubinova, S.; Hobzova, R.; Stranska, D.; Kozlik, P.; Bosakova, Z.; Marekova, D.; Holan, V.; Sykova, E.; Michalek, J. Controlled Gentamicin Release from Multi-Layered Electrospun Nanofibrous Structures of Various Thicknesses. *Int. J. Nanomed.* **2012**, *7*, 5315–5325.

(25) Besra, L.; Liu, M. A Review on Fundamentals and Applications of Electrophoretic Deposition (EPD). *Prog. Mater. Sci.* **2007**, *52*, 1–61.

(26) Zhitomirsky, D.; Roether, J. A.; Boccaccini, A. R.; Zhitomirsky, I. Electrophoretic Deposition of Bioactive Glass/Polymer Composite Coatings with and without HA Nanoparticle Inclusions for Biomedical Applications. *J. Mater. Process. Technol.* **2009**, *209*, 1853–1860.

(27) Yang, C. C.; Lin, C. C.; Yen, S. K. Electrochemical Deposition of Vancomycin/Chitosan Composite on Ti Alloy. *J. Electrochem. Soc.* **2011**, *158*, E152–E158.

(28) Patel, K. D.; El-Fiqi, A.; Lee, H. Y.; Singh, R. K.; Kim, D. A.; Lee, H. H.; Kim, H. W. Chitosan-Nanobioactive Glass Electrophoretic Coatings with Bone Regenerative and Drug Delivering Potential. *J. Mater. Chem.* **2012**, *22*, 24945–24956.

(29) Patel, K. D.; Singh, R. K.; Lee, E.-J.; Han, C.-M.; Won, J.-E.; Knowles, J. C.; Kim, H.-W. Tailoring Solubility and Drug Release from Electrophoretic Deposited Chitosan–Gelatin Films on Titanium. *Surf. Coat. Technol.* **2014**, *242*, 232–236.

(30) Wang, Y.; Zhang, W.; Zhang, J.; Sun, W.; Zhang, R.; Gu, H. Fabrication of a Novel Polymer-Free Nanostructured Drug-Eluting Coating for Cardiovascular Stents. *ACS Appl. Mater. Interfaces* **2013**, *5*, 10337–10345.

(31) Liu, Y.; Wang, W.; Acharya, G.; Shim, Y.-B.; Choe, E.; Lee, C. Advanced Stent Coating for Drug Delivery and In Vivo Biocompatibility. *J. Nanopart. Res.* **2013**, *15*, 1–16.

(32) Simchi, A.; Pishbin, F.; Boccaccini, A. R. Electrophoretic Deposition of Chitosan. *Mater. Lett.* **2009**, *63*, 2253–2256.

(33) Pishbin, F.; Simchi, A.; Ryan, M. P.; Boccaccini, A. R. A Study of the Electrophoretic Deposition of Bioglass® Suspensions Using the Taguchi Experimental Design Approach. *J. Eur. Ceram. Soc.* **2010**, *30*, 2963–2970.

(34) Pishbin, F.; Simchi, A.; Ryan, M. P.; Boccaccini, A. R. Electrophoretic Deposition of Chitosan/45S5 Bioglass® Composite Coatings for Orthopaedic Applications. *Surf. Coat. Technol.* **2011**, *205*, 5260–5268.

(35) Pishbin, F.; Mourino, V.; Gilchrist, J. B.; McComb, D. W.; Kreppel, S.; Salih, V.; Ryan, M. P.; Boccaccini, A. R. Single-Step electrochemical Deposition of Antimicrobial Orthopaedic Coatings Based on a Bioactive Glass/Chitosan/Nano-Silver Composite System. *Acta Biomater.* **2013**, *9*, 7469–7479.

(36) Sigma-Aldrich, Gentamicin Solution G1272 Product Information: http://www.sigmaaldrich.com/etc/medialib/docs/Sigma/Product_Information_Sheet/g1272pis.Par.0001.File.tmp/g1272pis.pdf; last accessed 2014/05/06.

(37) Kokubo, T.; Takadama, H. How Useful Is SBF in Predicting In Vivo Bone Bioactivity? *Biomaterials* **2006**, *27*, 2907–2915.

(38) Hench, L. L. In *Biomaterials, Artificial Organs and Tissue Engineering*; Hench, L. L., Jones, J. R., Eds.; Woodhead Publishing Limited: Cambridge, UK, 2005; Chapter 12, pp 119–127.

(39) Sampath, S. S.; Robinson, D. H. Comparison of New and Existing Spectrophotometric Methods for the Analysis of Tobramycin and Other Aminoglycosides. *J. Pharm. Sci.* **1990**, *79*, 428–431.

(40) Clinical and Laboratory Standards Institute, CLSI M02-A10: Performance Standards for Antimicrobial Disk Susceptibility Tests; Approved Standard -Tenth Edition, Published 01/07/2010, Wayne, PA.

(41) Paluszkiwicz, C.; Stodolak, E.; Hasik, M.; Blazewicz, M. FT-IR Study of Montmorillonite–Chitosan Nanocomposite Materials. *Spectrochim. Acta, Part A* **2011**, *79*, 784–788.

(42) Kontonasaki, E.; Zorba, T.; Papadopoulou, L.; Pavlidou, E.; Chatzistavrou, X.; Paraskevopoulos, K.; Koidis, P. Hydroxy Carbonate Apatite Formation on Particulate Bioglass® In Vitro as a Function of Time. *Cryst. Res. Technol.* **2002**, *37*, 1165–1171.

(43) Coates, J. In *Encyclopedia of Analytical Chemistry: Applications, Theory and Instrumentation*; Meyers, R. A., Ed.; Wiley: Hoboken, NJ, 2006; pp 10815–10837.

(44) Wanjun, T.; Cunxin, W.; Donghua, C. Kinetic Studies on the Pyrolysis of Chitin and Chitosan. *Poly. Degrad. Stab.* **2005**, *87*, 389–394.

(45) Mourino, V.; Newby, P.; Pishbin, F.; Cattalini, J. P.; Lucangioli, S.; Boccaccini, A. R. Physicochemical, Biological and Drug-Release Properties of Gallium Crosslinked Alginate/Nanoparticle Bioactive Glass Composite Films. *Soft Matter* **2011**, *7*, 6705–6712.

(46) Jones, J. R.; Sepulveda, P.; Hench, L. L. Dose-Dependent Behavior of Bioactive Glass Dissolution. *J. Biomed. Mater. Res.* **2001**, *58*, 720–726.

(47) Li, P.; Zhang, F. The Electrochemistry of a Glass Surface and Its Application to Bioactive Glass in Solution. *J. Non-Cryst. Solids* **1990**, *119*, 112–118.

(48) Pishbin, F. Development and Characterisation of Bioactive Coatings Based on Biopolymer and Bioactive Glass Obtained by Electrochemical Means. *Ph.D. Thesis*, Imperial College London, London, UK, 2013.

(49) Baudoux, P.; Bles, N.; Lemaire, S.; Mingeot-Leclercq, M.; Tulkens, P.; Van Bambeke, F. Combined Effect of pH and Concentration on the Activities of Gentamicin and Oxacillin Against *Staphylococcus Aureus* in Pharmacodynamic Models of Extracellular and Intracellular Infections. *J. Antimicrob. Chemother.* **2007**, *59*, 246–253.

(50) Schafer, T. W. Evaluation of Gentamicin for Use in Virology and Tissue Culture. *Appl. Environ. Microbiol.* **1972**, *23*, 565–570.

(51) Xue, J. M.; Shi, M. PLGA/Mesoporous Silica Hybrid Structure for Controlled Drug Release. *J. Controlled Release* **2004**, *98*, 209–217.

(52) Kim, H. M.; Kishimoto, K.; Miyaji, F.; Kokubo, T.; Yao, T.; Suetsugu, Y.; Tanaka, J.; Nakamura, T. Composition and Structure of Apatite Formed on Organic Polymer in Simulated Body Fluid with a High Content of Carbonate Ion. *J. Mater. Sci.: Mater. Med.* **2000**, *11*, 421–426.

(53) Barrère, F.; Layrolle, P.; van Blitterswijk, C. A.; de Groot, K. Biomimetic Calcium Phosphate Coatings on Ti6Al4V: a Crystal Growth Study of Octacalcium Phosphate and Inhibition by Mg^{2+} and HCO_3^- . *Bone* **1999**, *25*, 107S–111S.

(54) Bohner, M.; Lemaire, J. Can Bioactivity Be Tested In Vitro with SBF Solution? *Biomaterials* **2009**, *30*, 2175–2179.

(55) Benson, J. R.; Hare, P. E. O-Phthalaldehyde: Fluorogenic Detection of Primary Amines in the Picomole Range. Comparison with Fluorescamine and Ninhydrin. *Proc. Natl. Acad. Sci. U.S.A.* **1975**, *72*, 619–622.

(56) Mario, G.; Gabriele, G. Mathematical Modelling and Controlled Drug Delivery: Matrix Systems. *Curr. Drug Delivery* **2005**, *2*, 97–116.

(57) Ehlert, N.; Badar, M.; Christel, A.; Lohmeier, S. J.; Luessenhop, T.; Stieve, M.; Lenarz, T.; Mueller, P. P.; Behrens, P. Mesoporous Silica Coatings for Controlled Release of the Antibiotic Ciprofloxacin from Implants. *J. Mater. Chem.* **2011**, *21*, 752–760.

(58) Campos, M. G. N.; Rawls, H. R.; Innocentini-Mei, L. H.; Satsangi, N. In Vitro Gentamicin Sustained and Controlled Release from Chitosan Cross-Linked Films. *J. Mater. Sci.: Mater. Med.* **2009**, *20*, 537–542.